DOI 10.48612/fpg/7k5k-zu86-nxhz

© *A. G. Luchinin**, *V. Yu. Kirillin*, 2022
© Translation from Russian: *N. V. Mironova*, 2022
Institute of Applied Physics, Russian Academy of Sciences, 603950, Ul'anova str., 46, Nizhny Novgorod, Russia
*E-mail: luch@ipfran.ru

CHARACTERISTICS OF THE IMAGE SYSTEM BASED ON PHOTON DENSITY WAVES IN OBSERVING UNDERWATER OBJECTS THROUGH A WAVED SURFACE

Received 10.11.2021; Revised 30.12.2021; Accepted 01.02.2022

Abstract

The wavy surface effect on the resolution of optical imaging systems employing narrow modulated probing beams is studied. Relations are formulated connecting the complex amplitudes of the photon density waves (propagating through the wavy interface and the water layer) to the main parameters of the problem. These relations consider the finite waves height and the change in the photon trajectory length due to random refraction of rays upon entering the water. The optical transfer function of the wavy surface and the beam scattering function averaged over the ensemble of surface waving realizations are introduced. The dependences of these functions on the surface waves integral parameters, namely, the elevations and slopes dispersions, are examined. The contributions of surface waving and water layer to the generation of optical transfer functions and to the overall signal level from an underwater object when it is imaged using photon density waves are estimated. It is shown that in a certain range of depths, spatial frequencies, and illumination beam modulation frequencies, the systems employing photon density waves can demonstrate advantages over the systems with stationary illumination.

Keywords: imaging systems, wavy surface, modulated transfer function, photon density waves, multiply scattering

© *А. Г. Лучинин**, *М. Ю. Кириллин*, 2022
© Перевод с русского: *Н. В. Миронова*, 2022
Институт прикладной физики РАН, 603950, ул. Ульянова, д. 46, г. Нижний Новгород, Россия
*E-mail: luch@ipfran.ru

ХАРАКТЕРИСТИКИ СИСТЕМЫ ВИДЕНИЯ НА ВОЛНАХ ФОТОННОЙ ПЛОТНОСТИ ПРИ НАБЛЮДЕНИИ ПОДВОДНЫХ ОБЪЕКТОВ ЧЕРЕЗ ВЗВОЛНОВАННУЮ ПОВЕРХНОСТЬ

Статья поступила в редакцию 10.11.2021, после доработки 30.12.2021, принята в печать 01.02.2022

Аннотация

Исследовано влияние взволнованной поверхности на разрешающую способность систем видения, использующих для подсветки узкие модулированные пучки. Сформулированы соотношения, связывающие комплексные амплитуды волн фотонной плотности, распространяющихся через взволнованную границу и слой воды, с основными параметрами задачи. Эти соотношения учитывают конечную высоту волн и изменение длины траекторий фотонов при случайном преломлении лучей при вхождении в воду Введены усредненные по ансамблю реализаций поверхностного волнения оптическая передаточная функция взволнованной поверхности и функция рассеяния пучка. Исследованы зависимости этих функций от интегральных параметров волнения — дисперсии возвышений и дисперсии уклонов. Выполнены оценки вкладов поверхностного волнения и слоя воды в формирование оптических передаточных функций и в общий уровень сигнала от подводного объекта при его наблюдении с применением волн фотонной плотности. Показано, что в некотором диапазоне глубин, пространственных частот и частот модуляции пучка подсветки системы с применением волн фотонной плотности могут иметь преимущества перед системами со стационарной подсветкой.

Ключевые слова: системы видения, взволнованная поверхность, оптическая передаточная функция, волны фотонной плотности, многократное рассеяние

Ссылка для цитирования: *Лучинин А.Г.*, *Кириллин М.Ю.* Характеристики системы видения на волнах фотонной плотности при наблюдении подводных объектов через взволнованную поверхность // Фундаментальная и прикладная гидрофизика. 2022. Т. 15, № 3. С. 125–136. doi:10.48612/fpg/7k5k-zu86-nxhz

For citation: *Luchinin A.G.*, *Kirillin V. Yu.* Characteristics of the Image System based on Photon Density Waves in Observing Underwater Objects through a Waved Surface. *Fundamental and Applied Hydrophysics*. 2022, 15, 3, 125–136. doi:10.48612/fpg/7k5k-zu86-nxhz

1. Introduction

In a number of papers, it has been shown in various approximations that the use of light beams power-modulated with high frequency as illumination for imaging in underwater imaging systems can increase the spatial resolution of such systems [1–4]. This effect is caused by the suppression of the diffuse variable component of radiation at the periphery of the illumination beam due to the interference of photon density waves during multiple dispersion in water. It was also confirmed by a series of laboratory experiments [5, 6]. In this regard, it is of interest to evaluate the possibility of using modulated illumination beams (photon density waves) for imaging while observing through a wavy surface. In relation to the photon density waves the wavy surface plays the role of a random phase screen that distorts the structure of the light field refracted by the surface and, as a result, the structure of the formed image. The fundamental characteristic of the imaging system is the optical transfer function (OTF), which determines the display of the observed object contrast in the form of an infinite target with a sinusoidal distribution of the reflection coefficient. For the first time, the imaging system OTF applied to observation through a wavy surface was introduced in the work [7]. The work showed that this function can be expressed in terms of the characteristic function of wave slopes in order to describe the image averaged over the ensemble of surface waving realizations. In the work [8] this result was generalized, considering the effects of multiple light scattering in water. This work showed that the average OTF of a system for observation through the wavy surface can be represented as a product of individual OTFs: surface OTF and the OTF of the water layer between the sea surface and the observation object, for example, the bottom. This result was obtained in the small angle approximation of the radiative transfer equation, which does not consider the spread of photons along the travel paths during multiple scattering. Similarly, in this approximation, the same effect was not taken into account due to the finite waves' height and the change in the photon trajectory length with random refraction upon entering the water. This study is focused on the assessment of these effects influence on the statistical characteristics of the OTF for imaging systems applied to wavy surface when using modulated illumination beams. The analysis will be based on the principles and analytical relations of the theory of image transfer in scattering media, formulated in the works [9–12].

2. Methods

2.1. Problem statement

Let us specify the observation scheme and some important parameters. Let the observation system be located at a height H above the average level of a wavy surface. Assuming that the radiation source and receiver are aligned in space, we set their coordinates in the horizontal plane as a vector $\mathbf{r}_S$. Let the observation object with a diffuse reflection coefficient $R(\mathbf{r})$ be located at a depth Z. Its image can be generated as a result of scanning the object with a narrow beam and reproducing the power of the signal reflected by the object in the receiving system as a function of the illumination beam axis position or the illumination beam direction. If the beam position in the object plane is set by the vector $\mathbf{r}_0$, the determination of the object optical image is reduced to calculating the signal power distribution $P_{ob}(\mathbf{r}_0)$ corresponding to the given distribution of the object's reflection coefficient $R(\mathbf{r})$. In the case of a smooth air-water interface the vector $\mathbf{r}_0$ is related to the direction of radiation by the relation $\mathbf{r}_0 = \mathbf{r}_S + \mathbf{n}_0(H + Z/m)$ (Fig. 1). Here $\mathbf{n}_0$ is the horizontal plane projection of the unit vector $\mathbf{n}$ which determines the direction of the illumination beam axis, and m is the refractive index of water.

In the general case of non-stationary illumination and arbitrary directivity patterns of the emitter and receiver, the equation relating the signal power $P_{ob}(\mathbf{r}_0, t)$ to the distribution $R(\mathbf{r})$, observation system parameters, and medium properties is [9]:

$$P_{ob}(\mathbf{r}_0,t) = \frac{\Sigma\Delta\Omega\left(1-R_{sf}\right)^2}{\pi m^2}\iiint\limits_{\infty} R(\mathbf{r})E_S(\mathbf{r}_0,\mathbf{r},Z,t')E_R(\mathbf{r}_0,\mathbf{r},Z,t-t')d\mathbf{r}dt', \quad (1)$$

where Σ and Ω are the area of the receiving aperture and the acceptance angle, respectively, m is the refractive index of water, R_{sf} is the surface reflection coefficient, which we assume to be independent of the rays' arriving angle within the field of view, $P^0(t)$ is the power of the radiation source, $E_S(\mathbf{r}_0, \mathbf{r}, Z, t)$ is the irradiance distribution generated by the probing beam, $E_R(\mathbf{r}_0, \mathbf{r}, Z, t)$ is a similar distribution generated by

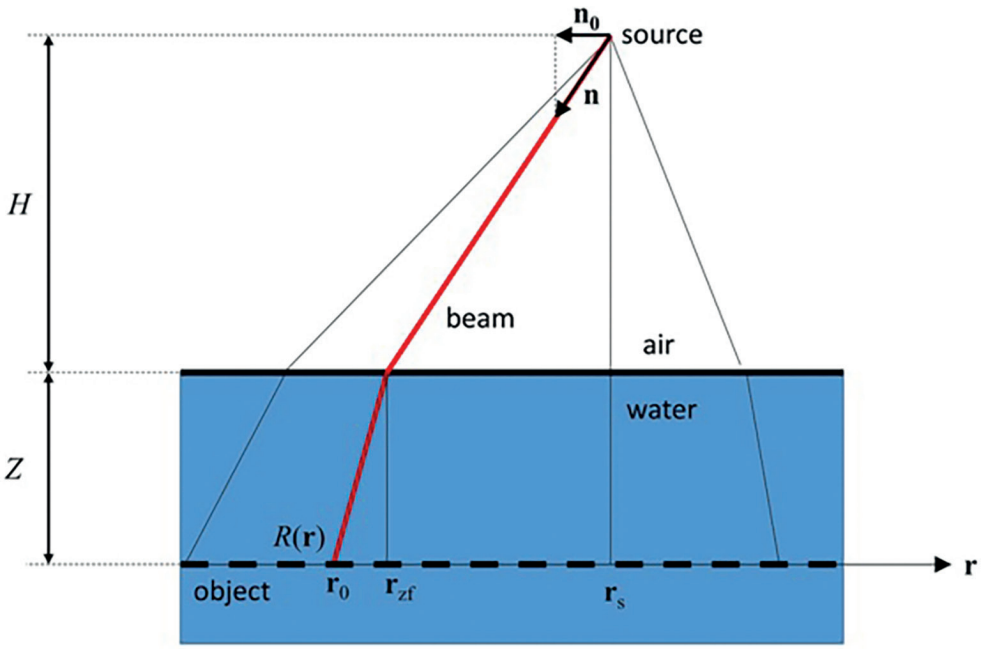

Fig. 1. Ray path diagram

a fictitious source with a unit of energy, with the same spatial and angular characteristics and time dependence (reproducing the impulse transient response of the signal receiving and processing system) as those of the receiver, and $\mathbf{r}_0$ is a vector describing the position of the illumination beam center and receiving diagram in the object plane. If the radiation source is modulated in time by a harmonic signal with frequency ω and the variable component of the signal at this frequency is detected in the receiver, then equation (1) can be transformed into:

$$P_{ob}(\mathbf{r}_0,\omega)=\frac{\Sigma\Delta\Omega P_{\omega}^{0}\left(1-R_{sf}\right)^{2}}{\pi m^{2}}\iint_{\infty}R(\mathbf{r})E_S(\mathbf{r}_0,\mathbf{r},Z,\omega)E_R(\mathbf{r}_0,\mathbf{r},Z,\omega)d\mathbf{r}, \tag{2}$$

where P_0^{ω} is the amplitude of the source power variable component. Next, we will specify the characteristics of the receiver and emitter. Let the receiver have a wide directivity pattern, which can be considered isotropic within the field of view. The emitter forms a narrow beam, which brightness' variable component can be approximated by delta functions in terms of spatial and angular variables:

$$I_S\left(\mathbf{r},\mathbf{n},\omega\right)=P_0^{\omega}\delta\left(\mathbf{r}-\mathbf{r}_S\right)\delta\left(\mathbf{n}-\mathbf{n}_0\right). \tag{3}$$

Since the light is refracted randomly upon entering the water, the integrands E_S and E_R in (2) are random, and the signal power P_{ob} is also a random variable. For a signal averaged over an ensemble of wavy surface realizations, the following relation is true:

$$\left\langle P_{ob}(\mathbf{r}_0,\omega)\right\rangle=\frac{\Sigma\Delta\Omega P_{\omega}^{0}\left(1-R_{sf}\right)^{2}}{\pi m^{2}}\iint_{\infty}R(\mathbf{r})\left\langle E_S(\mathbf{r}_0,\mathbf{r},Z,\omega)E_R(\mathbf{r}_0,\mathbf{r},Z,\omega)\right\rangle d\mathbf{r}. \tag{4}$$

Further on we will neglect the correlations between E_S and E_R functions. Their influence on the imaging system characteristics, in particular, on the form of the averaged OTF, was studied in the work [13]. The estimates made in this work show that the correlation effects lead to a noticeable change in the OTF only in the region of high spatial frequencies, where the contrast of the formed image is low. Therefore, here we will neglect this effect and assume that the following equality is true:

$$\left\langle E_S(\mathbf{r}_0,\mathbf{r},Z,\omega)E_R(\mathbf{r}_0,\mathbf{r},Z,\omega)\right\rangle = \left\langle E_S(\mathbf{r}_0,\mathbf{r},Z,\omega)\right\rangle\left\langle E_R(\mathbf{r}_0,\mathbf{r},Z,\omega)\right\rangle. \quad (5)$$

It is appropriate to note that for other methods of imaging (for example, during synchronous scanning with a beam and a narrow receiving diagram), these estimates obtained in the work [13] and the general analysis of the surface effect require refinement.

Let us introduce explicitly the dependences of functions on the waving characteristics. For simplicity, we confine ourselves to analyzing the properties of these functions in the central part of the image, assuming that their structure does not change when the coordinate $\mathbf{r}_0$ is changed. In this case, the generated signal depends only on the difference between $\mathbf{r}_0$ and **r.** This is equivalent to neglecting the effects associated with violation of the image isoplanatism and allows us to implement $\mathbf{r}_0$=0, $\mathbf{n}_0$=0 to (4) in order to simplify the formulas. In this approximation, in the absence of waving (in the case of a smooth surface), the distribution of the complex amplitude of the irradiance's variable component E_S at depth Z can be represented as the product

$$E_S\left(\mathbf{r},Z,\omega\right) = e\left(\mathbf{r},Z,\omega\right)\exp\left(-i\frac{\omega}{c}\left(H+mZ\right)\right), \quad (6)$$

where c is the speed of light. The value $\varphi_0 = -\frac{\omega}{c}\left(H+mZ\right)$ describes the regular (geometric) phase incursion, and the function $e(\mathbf{r}, Z, \omega)$ describes the irradiance distribution in the photon density wave generated by a point mono-directional source located at the interface in the Z = const plane, taking into account the additional phase incursion due to multiple scattering in water. When the beam is refracted on a wavy surface, the direction of its propagation in water and the distance to its intersection with the Z = const plane are changed. Therefore, the relation (6) must be transformed as follows:

$$E_S\left(\mathbf{r},Z,\omega\right) = e\left(\mathbf{r}+Zq\boldsymbol{\eta},Z,\omega\right)\exp\left(-i\frac{\omega}{c}\left(H-\xi+m\left(Z+\xi+Zq^2\frac{\eta^2}{2}\right)\right)\right), \quad (7)$$

where ξ is a random elevation of the surface at the point of beam entrance to water, and $\eta = -\nabla\xi$ is the surface slope at the same point, $q = (m-1)/m$. When transforming the arguments of the function $E_S(\bullet)$ into (7), the following inequalities were assumed to be satisfied: $q|\boldsymbol{\eta}| \ll 1$ and $\xi \ll Z$. Let us introduce the spectrum of the transverse distribution of irradiance $e(\mathbf{r}, Z, \omega)$ in the absence of waving:

$$\Phi(\mathbf{k},Z,\omega) = \left(2\pi\right)^{-2}\iint e\left(\mathbf{r},Z,\omega\right)\exp\left(-i\mathbf{k}\mathbf{r}\right)d\mathbf{r}. \quad (8)$$

Assuming **r** and η to be independent variables, we introduce, similarly to (8), the Fourier transform of the function $E_S(\mathbf{r}, Z, \omega)$:

$$\Phi_S(\mathbf{k},Z,\omega) = \left(2\pi\right)^{-2}\iint e_S\left(\mathbf{r},Z,\omega\right)\exp\left(-i\mathbf{k}\mathbf{r}\right)d\mathbf{r}. \quad (9)$$

As follows from (7) and (8),

$$\Phi_S(\mathbf{k},Z,\omega) = \Phi(\mathbf{k},Z,\omega)\exp\left(iZq\mathbf{k}\boldsymbol{\eta} - i\frac{\omega}{c}\left(H-\xi+m\left(Z+\xi+Zq^2\frac{\eta^2}{2}\right)\right)\right). \quad (10)$$

Averaging (10) over an ensemble of surface waving realizations, we obtain an equation for the statistically average spatial spectrum of the irradiance's variable component:

$$\left\langle\Phi_S(\mathbf{k},Z,\omega)\right\rangle = \iiint\Phi_S(\mathbf{k},Z,\omega,\xi,\boldsymbol{\eta})W\left(\xi,\boldsymbol{\eta}\right)d\xi d\boldsymbol{\eta}, \quad (11)$$

where $W(\xi, \eta)$ is the joint function of elevations and slopes probability distribution. The one-point distribution function of elevations and slopes applicable in (11) can be represented as a product $W(\xi, \eta) = W(\xi)W(\eta)$. This equality is valid due to the equality to zero of the distribution moments $\left\langle\xi(\mathbf{r}_1)\eta_x(\mathbf{r}_2)\right\rangle$, and $\left\langle\xi(\mathbf{r}_1)\eta_y(\mathbf{r}_2)\right\rangle$, if $\mathbf{r}_1 = \mathbf{r}_2$.

Assuming further that the waves are normal and isotropic, we represent the elevations and slopes distribution functions in the form of Gaussian functions, i.e.: $W\left(\xi\right) = \frac{1}{\sqrt{2\pi\sigma_\xi^2}}\exp\left(-\frac{\xi^2}{2\sigma_\xi^2}\right)$ and $W\left(\eta\right) = \frac{1}{2\pi\sigma_\eta^2}\exp\left(-\frac{\eta^2}{2\sigma_\eta^2}\right)$.

Then from (4) and (5) we obtain a formula for the average value of the function Φ_S:

$$\left\langle \Phi_S(\mathbf{k},Z,\omega)\right\rangle = \frac{\Phi(\mathbf{k},Z,\omega)}{1+i\kappa Z q^2\sigma_\eta^2}\exp\left(-i\varphi_0 - \frac{\kappa^2 q^2\sigma_\xi^2}{2} - \frac{k^2Z^2q^2\sigma_\eta^2}{2\left(1+i\kappa Z q^2\sigma_\eta^2\right)}\right), \tag{12}$$

where κ is the wavenumber in water ($\kappa = m\omega/c$), σ_ξ^2 and σ_η^2 are the dispersions of surface elevations and slopes, respectively. Thus, the spatial spectrum of the irradiance's variable component $\left\langle E_S\left(\mathbf{r},Z,\omega\right)\right\rangle$ can be represented as the product of the spectrum in the absence of waves and additional function describing the effect of waving, which is reduced not only to the spectrum attenuation at high spatial frequencies, but also to the general attenuation of the signal due to a random phase change at the final height of surface waves.

Let us take a look at the function $\left\langle E_R\left(\mathbf{r}_0,\mathbf{r},Z,\omega\right)\right\rangle$. Considering the approximations introduced above, this function can be represented as follows:

$$\left\langle E_R\left(\mathbf{r}_0,\mathbf{r},Z,\omega\right)\right\rangle = \frac{1}{\Delta\Omega}\iint\left\langle e_S\left(\mathbf{r}+\mathbf{n}(H+Z/m),Z,\omega\right)\right\rangle d\mathbf{n} = \frac{\left(2\pi\right)^2\left\langle\Phi_S\left(k=0,Z,\omega\right)\right\rangle}{\Delta\Omega\left(H+Z/m\right)^2}. \tag{13}$$

Since $\left\langle E_S(\mathbf{r}_0,\mathbf{r},Z,\omega)\right\rangle = \iint\left\langle\Phi_S\left(k,Z,\omega\right)\right\rangle\exp\left(i\mathbf{k}\left(\mathbf{r}-\mathbf{r}_0\right)\right)d\mathbf{k}$, equation (2) can be presented in the following form:

$$\left\langle P_{ob}(\mathbf{r}_0,\omega)\right\rangle = \frac{\Sigma\left(2\pi\right)^2 P_\omega^0\left(1-R_{sf}\right)^2\left\langle\Phi_S\left(k=0,Z,\omega\right)\right\rangle}{\pi m^2\left(H+Z/m\right)^2}\iint\limits_\infty R(\mathbf{r})\iint\left\langle\Phi_S\left(k,Z,\omega\right)\right\rangle\exp\left(i\mathbf{k}\left(\mathbf{r}-\mathbf{r}_0\right)\right)d\mathbf{k}d\mathbf{r}. \tag{14}$$

For a homogeneously reflecting object (the bottom with an equal distribution of the reflection coefficient R_0), from (14) follows the formula for the complex amplitude of the received signal:

$$\left\langle P_{ob}(\omega)\right\rangle = \frac{\Sigma R_0 P_\omega^0\left(1-R_{sf}\right)^2\left(2\pi\right)^4\left\langle\Phi_S\left(k=0,Z,\omega\right)\right\rangle^2}{\pi m^2\left(H+Z/m\right)^2}. \tag{15}$$

Its absolute value is determined by the following equation:

$$\left|\left\langle P_{ob}(\omega)\right\rangle\right| = \frac{\Sigma R_0 P_\omega^0\left(1-R_{sf}\right)^2\left(2\pi\right)^4\left|\left\langle\Phi\left(0,Z,\omega\right)\right\rangle\right|^2\exp\left(-\kappa^2q^2\sigma_\xi^2\right)}{\pi m^2\left(H+Z/m\right)^2\left(1+\left(\kappa Z q^2\sigma_\eta^2\right)^2\right)}. \tag{16}$$

Thus, the influence of waves on the overall level of the reflected signal leads to the exponential attenuation of the signal with increasing frequency due to its misphasing at a finite wave height and to the power attenuation due to misphasing at the angular spread of the beams. The OTF characterizes contrast transfer during the generation of the object image in the form of a target with sinusoidal reflection coefficient as a function of its spatial frequency. Therefore, after substituting the distribution $R(\mathbf{r})$ in the form of a harmonic function with spatial frequency $\mathbf{k}$ to (14) and performing some simple transformations, it is easy to obtain a formula for the formed image contrast:

$$K_{ob} = \left(P_{ob}^{\max} - P_{ob}^{\min}\right)/\left(P_{ob}^{\max} + P_{ob}^{\min}\right) = K_0\Theta_{tot}\left(\mathbf{k},Z,\omega\right), \tag{17}$$

where $P_{ob}^{\max}$ and $P_{ob}^{\min}$ are the complex amplitudes of the signals when the illumination beam is oriented to the object points with the maximum and minimum reflection coefficient, respectively, K_0 is the initial or true contrast of the target, $\Theta_{tot}(\mathbf{k}, Z, \omega)$ is the observation system OTF, which can be represented as a product of the independently calculated OTFs of the water layer and the surface:

$$\Theta_{tot}\left(\mathbf{k},Z,\omega\right) = \Theta_{wat}\left(\mathbf{k},Z,\omega\right)\Theta_{sf}\left(\mathbf{k},Z,\omega\right), \tag{18}$$

$$\Theta_{wat}\left(\mathbf{k},Z,\omega\right) = \frac{\Phi\left(\mathbf{k},Z,\omega\right)}{\Phi\left(\mathbf{k}=0,Z,\omega\right)}, \tag{19}$$

$$\Theta_{sf}\left(\mathbf{k},Z,\omega\right) = \exp\left(-\frac{k^2Z^2q^2\sigma_\eta^2}{2\left(1+i\kappa Z q^2\sigma_\eta^2\right)}\right). \tag{20}$$

Given ω = 0, equation (18) coincides with the result obtained earlier in the small-angle approximation as applied to stationary fields [8].

Obtained relations enable us to estimate the effect of various factors on the observation system characteristics and compare the contributions of the wavy surface and scattering in water to the signal generation.

2.2. Optical transfer function of wavy surface

Before proceeding to the comparison of the losses introduced by the surface and the water layer to the formation of the joint OTF and to the overall signal level, let us consider the surface OTF separately, assuming that the depth Z is not large and, hence, the water layer OTF can be considered constant. In this case, for isotropic waves

$$\Theta_{sf}\left(k,Z,\omega\right)=\left|\Theta_{sf}\left(k,Z,\omega\right)\right|\exp\left(i\varphi_{sf}\left(k,Z,\omega\right)\right), \tag{21}$$

$$\left|\Theta_{sf}\left(k,Z,\omega\right)\right|=\exp\left(-\frac{k^2\delta}{2}\right), \tag{22}$$

$$\varphi_{sf}\left(k,Z,\omega\right)=\frac{k^2\kappa Z q^2\sigma_\eta^2\delta}{2}, \tag{23}$$

where parameter $\delta=\dfrac{Z^2q^2\sigma_\eta^2}{1+\kappa^2Z^2q^4\sigma_\eta^4}$ defines the width of the surface OTF. As follows from (21)—(23), the wavenumber κ or frequency ω is a significant parameter of the surface OTF. The shape of the OTF absolute value and phase is of particular interest for asymptotically large values of these parameters, when the following inequality holds:

$$\kappa^2Z^2q^4\sigma_\eta^4\gg 1. \tag{24}$$

Under this condition, (22) and (23) can be represented as follows:

$$\left|\Theta_{sf}\left(k,Z,\omega\right)\right|=\exp\left(-\frac{k^2}{2\kappa^2q^2\sigma_\eta^2}\right), \tag{25}$$

$$\varphi_{sf}\left(k,Z,\omega\right)=-\frac{k^2Z}{2\kappa}. \tag{26}$$

As follows from (22), the surface OTF absolute value is invariant in respect to k/κ and does not depend on depth. Its dependence the surface waving magnitude is also uncommon: the exponent in (25) is inversely proportional to the slopes dispersion. In fact, this means that the beam scattering by the high-frequency variable component decreases with slopes increase. This effect is, to a certain extent, analogous to the suppression of the variable component of radiation at the periphery of the beam in water due to interference effects at multiple scattering [3, 4]. The OTF phase, in contrast to its absolute value, does not depend on the slopes and is proportional to the product of the parameter k/κ and the angular frequency kZ, when (24) is satisfied. The presence of the exponent maximum in (22) with a change in the slopes dispersion is another interesting feature of the surface OTF. This maximum is reached under the following condition:

$$q^2\sigma_\eta^2=\left(\kappa Z\right)^{-2}. \tag{27}$$

In this case, as follows from (23)—(25), the complex surface OTF takes the following form:

$$\Theta_{sf}\left(k,Z,\omega\right)=\exp\left(-\frac{k^2Z\left(1+i\right)}{4\kappa}\right). \tag{28}$$

It is clear that condition (27) (given the slopes dispersion has a fixed value) can be realized with a change in frequency ω only at fixed depth.

When the inequality opposite to (24) is satisfied, the surface OTF transforms into the OTF for the stationary object.

2.3. Beam Scattering Function

Let us introduce another characteristic, which is important for evaluating the effect of the wavy surface on the capabilities of imaging systems used for this type of surface. The beam scattering function (BSF) is Fourier conjugated with the OTF. This function (normalized to its value considering $r = 0$), in accordance with (18)—(20), has the following form:

$$\Pi_{sf}\left(r,Z,\omega\right)=\exp\left(-\frac{r^2\left(1-i\kappa Zq^2\sigma_\eta^2\right)}{2Z^2q^2\sigma_\eta^2}\right). \quad (29)$$

Relation (29) shows that BSF of a wavy surface on photon density waves is a function oscillating along r axis with an envelope matching stationary beam BSF. The BSF oscillation period does not depend on waving magnitude and is equal to $\sqrt{2\lambda Z}$, where λ is the length of the photon density wave. Thus, the average irradiance distribution in the photon density wave on Z = const plane is similar to a diffraction pattern with the main maximum width inversely proportional to the wave frequency and, again, independent of the waving magnitude. A simple explanation for this effect is that relation (29) describes the average over the ensemble of waving realizations and "instant" distribution of the irradiance's variable component with a phase counted from the phase at $r = 0$. The narrowing of the main maximum with increasing the wave frequency, regardless of the waving magnitude, leads to the features of the asymptotic behavior of the surface OTF described above.

The obtained dependences of the BSF on the problem parameters are quite predictable, since the average brightness distribution of the photon density wave under the surface is similar to the distribution in a spherical wave with the phase front center at Z = 0 and the amplitude with angle modulated by slopes distribution function.

Note that the above results can be obtained in a shorter, but less correct way: by formulating an equation for the function $\left\langle E_S(\mathbf{r}_0,\mathbf{r},Z,\omega)\right\rangle$ under boundary conditions corresponding to the average beam spread in directions determined by the slopes distribution function. The use of signal (2) as the initial equation for the random realization is necessary for correct transition to statistical characteristics, considering the finite wave height and solving the problems in a more complex setting, for example, at the finite beam width, its oblique incidence and (or) while studying the second statistical moments of the field. In this case, it is required to involve information about the two-point joint distribution functions of the surface elevations and slopes.

3. Results

3.1. Estimation of the average signal value

Although the obtained formulas describing the average signal value and the surface OTF are quite simple, it is good for clarity to provide their graphic view. It follows from (16) that the assessment of the influence of the observation path parameters on the average signal amount is reduced to the calculation of the following function:

$$K\left(Z,\omega\right)=K_{wat}\left(Z,\omega\right)K_{sf}\left(Z,\omega\right), \quad (30)$$

where $K_{wat}=\left|\Phi\left(0,Z,\omega\right)\right|^2$, and $K_{sf}=\dfrac{\exp\left(-\kappa^2q^2\sigma_\xi^2\right)}{1+\left(\kappa Zq^2\sigma_\eta^2\right)^2}$. The function Φ(0, Z, ω) can be calculated using the Monte Carlo statistical simulation method (its details in relation to the underwater distribution path of the light beam are described in [3, 4]). The influence of the surface on the amount of signal reflected from the homogeneous object can be estimated using data on the statistical characteristics of surface waves. Vast literature is devoted to the problem of analytical description of these characteristics. Here we will use the data of monograph [14], in which generalized data on the integral characteristics of waves (in particular, on the values σ_ξ^2 and σ_η^2) are given based on the analysis of various models of the surface waves spectrum. For estimates we will use specific data for the moderate near-water wind speed V = 5 m/s. According to [14], with this wind value σ_ξ^2 = = 0.0054 m^2 and σ_η^2 = 0.0215 rad^2 The slopes dispersion value equal to 0.0215 is the average for two orthogonal directions in respect to the wind speed vector.

The results of calculating K_{wat} and K_{sf} functions for these parameter values, depending on the frequency, are shown in Fig. 2.

As can be seen from this figure, the surface factor in the high frequency range is most significant for estimating the signal level. At the same time, the greatest contribution to the signal attenuation is made by the misphasing effect of the field's variable component due to the finite height of surface waves.

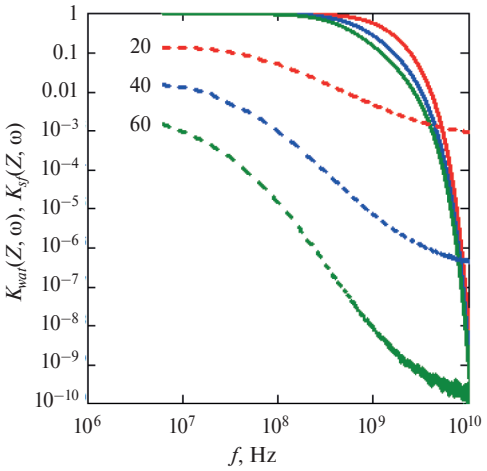

Fig. 2. Dependence of K_{wat} (dashed curves) and K_{sf} (solid curves) functions on the frequency $f = \omega/2\pi$ for depths Z equal to 20, 40 and 60 m. When calculating K_{wat} function, water scattering and absorption coefficients were considered to be equal to 0.16 1/m and 0.04 1/m, respectively

3.2. Estimation of optical transfer functions of water layer and surface

As mentioned above, the value δ characterizes the OTF width as a function of the spatial frequency and actually determines the range of resolved spatial frequencies. Therefore, before proceeding to a comparative assessment of the surface and the water layer contributions to the joint OTF creation, we will give examples of this value dependence on the main problem parameters.

Fig. 3–5 demonstrate the main features of the surface OTF listed in section 2.2: the appearance of the parameter δ maximum with a change in slopes dispersion at a certain combination of frequency and depth, its decreasing with the increase of slopes dispersion, and its independence from depth at high frequencies. It is appropriate to note that during the change in slopes dispersion parameter δ maximum is in the range of the values specific to the sea waves at moderate near-water wind speeds.

In the work [15], the results of Monte Carlo simulation of the water layer OTF on photon density waves were presented. These results can be compared with the results of the surface OTF calculation, performed according to the formula (8). Fig. 6 and 7 show the examples of calculating the surface and the water layer OTF absolute value for two depths and four frequencies of the photon density wave.

From the curves in these figures one can assess the relative contribution of scattering on the wavy surface and multiple scattering in the water column to the resolution of imaging systems when observing underwater objects from the atmosphere. After comparing the curves in these figures, we can conclude that the loss in resolution of high spatial frequencies when observing at photon density waves through a wavy surface is primarily determined by the waves, except for the region of very high beam modulation frequencies (~10^{10} Hz),

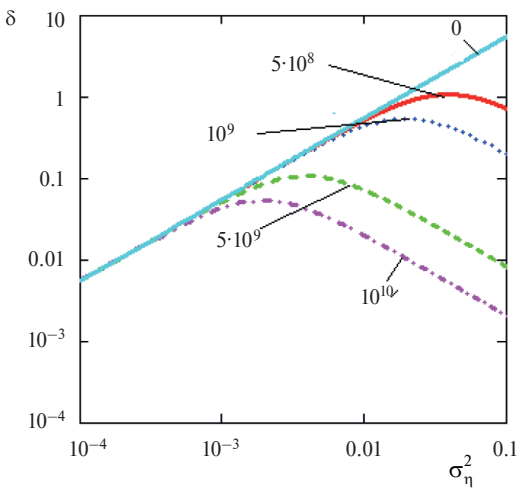

Fig. 3. Dependence of the parameter δ on the slopes dispersion for the depth Z = 30 m. The numbers indicate the frequency of the photon density wave in Hz

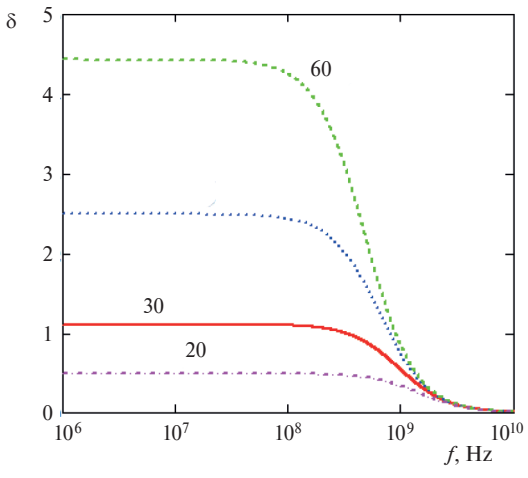

Fig. 4. Dependence of the parameter δ on the frequency at fixed depths (shown by numbers in meters). $\sigma_\eta^2 = 0.0215$ rad^2

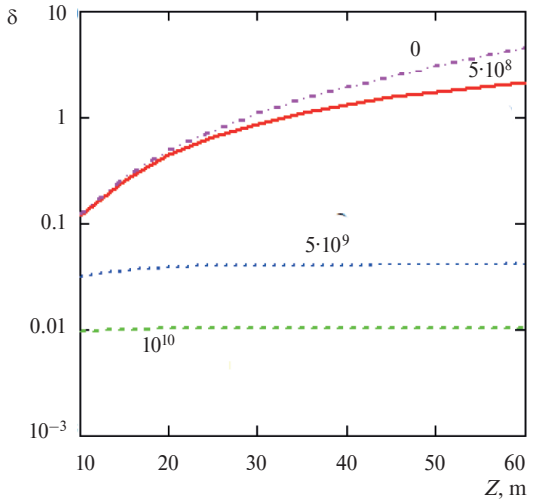

Fig. 5. Dependence of the parameter δ on the depth at fixed frequencies (shown by numbers in Hz). $\sigma_\eta^2 = 0.0215$ rad^2

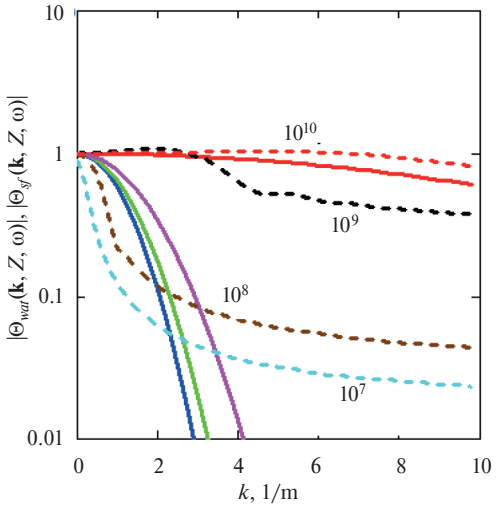

Fig. 6. The surface (solid curves) and the water layer (dashed curves) OTF absolute values at photon density waves of different frequencies (numbers in Hz) at a depth of $Z = 30$ m

where the contributions of the surface and the water layer are compared. At the same time, as follows from presented figures, in the region of relatively low spatial frequencies and at relatively low beam modulation frequencies the determining factor in the loss of contrast is multiple scattering in water.

3.3. Estimation of the signal amount when observing the test object

Generally speaking, the above estimates of the surface waves influence on the OTF properties of the surface systems for observing underwater objects on photon density waves are not sufficient for assessing the visibility of the objects. The calculation of the observation system OTF is necessary and sufficient in the case, when the possibility of observation is limited by the contrast sensitivity of the receiver. However, in some cases, the possibilities of observation (range and spatial resolution) are limited by the energy potential of the system. Then the determining value is not the contrast of the observed test object in the form of a target with a sinusoidal distribution of the reflection coefficient. It is the difference in signal levels when the illumination beam is oriented to the light and dark bands, which should exceed the noise level in the receiver. Here we provide an estimate of the surface and water column effect on this difference. Let us assume that the reflection coefficient of the test object is given as follows:

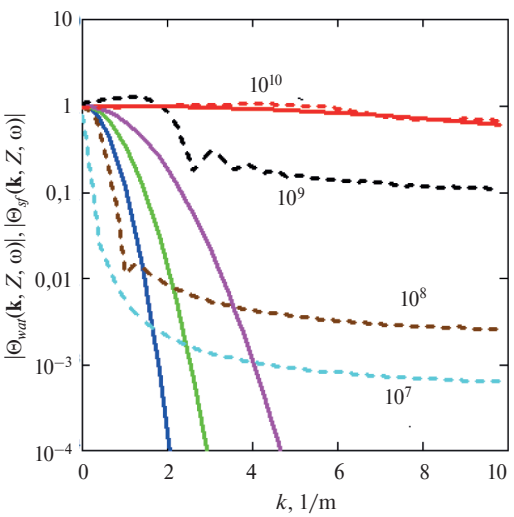

Fig. 7. The surface (solid curves) and the water layer (dashed curves) OTF absolute values at photon density waves of different frequencies (numbers in Hz) at a depth of $Z = 60$ m

$$R_{ob}(\mathbf{r}) = R_0\left(1 + K_0\cos(\mathbf{k}_0\mathbf{r})\right), \tag{31}$$

where R_0 is the average reflection coefficient and K_0 is the initial (true) contrast. Let us estimate the difference in signal levels when the illumination beam is directed to the point $\mathbf{r} = 0$ and to the point shifted by a distance equal to the half-period of the structure along the direction $\mathbf{k}_0$.

After substituting (31) into (14) we obtain the following relation for the absolute value of the signal difference:

$$\left|\Delta P_{ob}\left(k_0, Z, \omega\right)\right| = A\sqrt{K\left(Z, \omega\right)}\Theta_{tot}\left(k_0, Z, \omega\right), \tag{32}$$

where coefficient A contains all problem parameters independent from the medium properties and surface waves (radiation power, observation geometry, true contrast of the test object, etc.). Fig. 8 and 9 show the results of the "cumulative" effect of the surface and the water layer on the signal level normalized to the value A.

These results show that there is a range of parameters (observation depths, spatial frequencies, photon density wave frequencies) where the use of high-frequency modulated illumination beams can give a noticeable gain in resolution and range (depth) of observation.

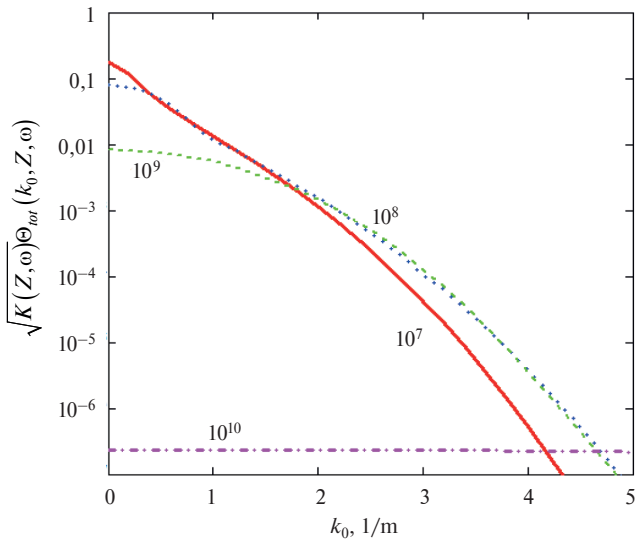

Fig. 8. Relative signal level for the observation depth of Z = = 30 m versus spatial frequency at different frequencies of the photon density wave (shown in Hz)

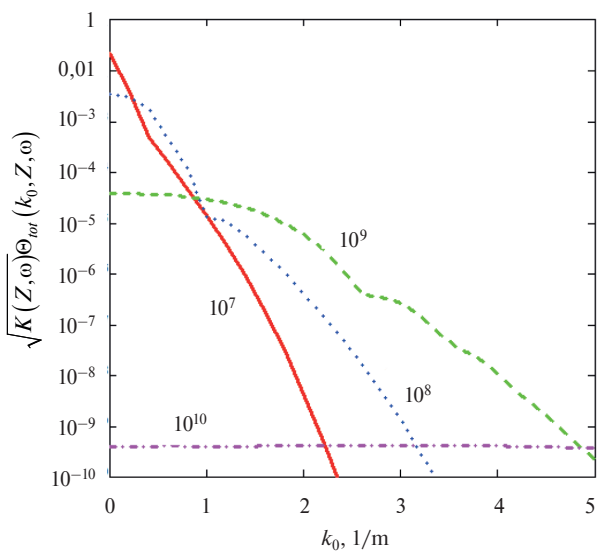

Fig. 9. Relative signal level for the observation depth of Z = = 60 m versus spatial frequency at different frequencies of the photon density wave (shown in Hz)

4. Discussion

The performed analysis of the wavy surface effect on the main characteristics of the imaging system based on photon density waves cannot claim to be a complete study of the problem. Since it is limited to establishing relationships between the average characteristics of the formed images and surface waves, its direct use for estimating the required parameters is possible only with a sufficiently long signal exposition. In addition, these results will be useful for assessing the possibility of detecting an object by one random realization of its image, if the calculations of the average image are supplemented with estimates of the dispersion of its fluctuations due to waving. These estimates were partially performed in [13] for the systems with stationary illumination. Paper [14] contains a review of fluctuation phenomena due to focusing of light by surface waves. However, as applied to the focusing of photon density waves generated by artificial source, this problem should be considered separately.

The second remark concerns the phase responses of the image. Our estimates mainly concern the frequency responses of the signals that form the image. In this case, it is implicitly assumed that during signal processing phase distortions can be eliminated by correcting the phase of the reference signal upon detection of the variable component in the receiving system. Of course, this issue also requires additional analysis when refining the image generation method, in particular, the method of scanning with an illumination beam.

5. Conclusion

The estimates of changes in the signal level and transmitted image contrast should be supplemented by calculations of the level of the image's noise components, which depend on the observation system energy potential and external conditions, in particular, on the level of background illumination. Therefore, the potential gain from waves influence reduction due to the use of modulated beams in imaging must also be evaluated considering the frequency dependence of these factors.

Note that an approach of waving effect reduction, alternative to the one considered above, was proposed in the work [16]. It is based on the formed image correction due to determining the refraction angle from the image shift of the back scattering impulsive noise. This work shows that the effect of beam spreading by surface waves can be reduced by an order of magnitude. Apparently, these approaches can be combined while using a pulsed illumination beam with intrapulse modulation by a complex high-frequency signal [17]. In this case, the depth resolution, enabling us to use the image of backscattering noise for estimating the refraction angle of the illumination beam, will be determined by the width of modulating signal band, and the use of a high-frequency modulation range will provide a gain in resolution due to interference effects during multiple scattering, which suppress the diffuse component of the radiation [15].

Acknowledgements

We thank L.S. Dolin for helpful advice that we used in our work.

Funding

This work was supported by the Ministry of Science and Higher Education of Russia (project 0030–2021–0006) and the Russian Foundation for Basic Research (project 19–02–00089a).

References

1. *Luchinin A.G.* Spatial spectrum of a narrow sine-wave-modulated light beam in an anisotropically scattering medium. *Izvestiya AN SSSR*, *Fizika Atmosfery i Okeana*. 1974, 10, 1312–1317 (In Russian).
2. *Remizovich V.S.*, *Rogozkin D.B.*, *Ryazanov M.I.* Propagation of a narrow modulated beam of light in a scattering medium taking into account fluctuations of photon traces at multiple scattering. *Izvestiya Vuzov*, *Radiofizika*. 1982, 25, 8, 891–898 (In Russian).
3. *Luchinin A.G.*, *Kirillin M. Yu*. Temporal and frequency characteristics of a narrow light beam in sea water. *Applied Optics*. 2016, 55, 7756–7762. doi:10.1364/AO.55.007756
4. *Luchinin A.G.*, *Kirillin M.Y.* Structure of a modulated narrow light beam in seawater: Monte Carlo simulation. *Izvestiya*, *Atmospheric and Oceanic Physics*. 2017, 53, 2, 242–249. doi:10.1134/S0001433817020086
5. *Gordeev L.B.*, *Luchinin A.G.*, *Shcegol'kov Yu.B.* Experimental studies of the structure of a narrow sine-wave-modulated light beam in a model anisotropically scattering medium. *Izvestiya AN SSSR*, *Fizika Atmosfery i Okeana*. 1975, 11, 50–53 (In Russian).
6. *Mullen L.*, *Laux A.*, *Concannon B.*, *Zege E.P.*, *Katsev I.L.*, *Prikhach A.S.* Amplitude-modulated laser imager. *Applied Optics*. 2004, **43,** 19, 3874–3892. doi:10.1364/ao.43.003874
7. *Mullamaa Yu.-A.R.* Effect of a rough sea surface on the visibility of submerged objects. *Izvestiya AN SSSR*, *Fizika Atmosfery i Okeana*. 1975, 11, 199–205 (In Russian).
8. *Luchinin A.G.* Some characteristics of the formation of a shelf image when it is observed through a wavy sea surface. *Izvestiya AN SSSR*, *Fizika Atmosfery i Okeana.* 1981, 17, 537–541 (In Russian).
9. *Dolin L.S.*, *Levin I.M.* Handbook of underwater vision theory. Leningrad, Gidrometeoizdat, 1991. 230 p. (In Russian).
10. *Dolin L.*, *Gilbert G.*, *Levin I.*, *Luchinin A.* Theory of imaging through wavy sea surface. *N. Novgorod*, *Institute of Applied Physics*, 2006. 180 p.
11. *Levin I.M.* Observation of objects illuminated by narrow light beam in scattering medium. *Izvestiya AN SSSR*, *Fizika Atmosfery i Okeana*. 1969, 5, 32–36 (In Russian).
12. *Bravo-Zhivotovsky D.M.*, *Dolin L.S.*, *Luchinin A.G.*, *Savel'ev V.A.* Problems of the theory of imaging in turbid media. *Izvestiya AN SSSR*, *Fizika Atmosfery i Okeana*. 1969, 5, 672–684 (In Russian).
13. *Veber V.L.*, *Luchinin A.G.* Influence of correlation effects on characteristics of bottom imaging through the rough surface of a body of water. *Izvestiya*, *Atmospheric and Oceanic Physics*. 2001, 37, 239–246.
14. *Walker R.E.* Marine Light Field Statistics. John Wiley&Sons, INC., 1994. 675 p.
15. *Luchinin A.G.*, *Kirillin M. Yu*. Nonstationary optical transfer functions of underwater imaging systems. *Applied Optics*. 2017, 56, 7518–7524. doi:10.1364/AO.56.007518
16. *Dolin L.S.*, *Luchinin A.G.* Water-scattered signal to compensate for the rough sea surface effect on bottom lidar imaging. *Applied Optics*. 2008, 47, 6871–6878. doi:10.1364/ao.47.006871
17. *Luchinin A.G.*, *Dolin L.S.* Model of an underwater imaging system with a complexly modulated illumination beam. *Izvestiya*, *Atmospheric and Oceanic Physics*. 2014, 50, 411–419. doi:10.1134/S0001433814040185

Литература

1. *Лучинин А.Г.* Пространственный спектр узкого синусоидально модулированного пучка света в анизотропно рассеивающей среде // Известия АН СССР. Физика атмосферы и океана. 1974. Т. 10, № 12. С. 1312–1317.
2. *Ремизович В.С.*, *Рогозкин Д.Б.*, *Рязанов М.И.* Распространение узкого модулированного пучка света в рассеивающей среде с учетом флуктуаций путей фотонов при многократном рассеянии // Известия вузов. Радиофизика. 1982. Т. 25, № 8. С. 891–898.
3. *Luchinin A.G.*, *Kirillin M. Yu.* Temporal and frequency characteristics of a narrow light beam in sea water // Applied Optics. 2016. Vol. 55, N 27. P. 7756–7762. doi:10.1364/AO.55.007756
4. *Лучинин А.Г.*, *Кириллин М.Ю.* Структура модулированного узкого пучка света в морской воде: моделирование методом Монте-Карло // Известия РАН. Физика атмосферы и океана. 2017. Т. 53, № 2. С. 275–284. doi:10.7868/S0002351517020080
5. *Гордеев Л.Б.*, *Лучинин А.Г.*, *Щегольков Ю.Б.* Экспериментальные исследования структуры узкого синусоидально модулированного пучка света в модельной анизотропно рассеивающей среде // Известия АН СССР. Физика атмосферы и океана. 1975. Т. 11, № 1 С. 86–89.
6. *Mullen L.*, *Laux A.*, *Concannon B.*, *Zege E.P.*, *Katsev I.L.*, *Prikhach A.S.* Amplitude-modulated laser imager // Applied Optics. 2004. Vol. 43, N 19. 3874–3892. doi:10.1364/ao.43.003874
7. *Мулламаа Ю.-А.Р.* Влияние взволнованной поверхности на видимость подводных объектов // Известия АН СССР. Физика атмосферы и океана. 1975. Т. 11, № 2. С. 199–205.
8. *Лучинин А.Г.* Некоторые закономерности формирования изображения шельфа при его наблюдении через взволнованную поверхность моря // Известия АН СССР. Физика атмосферы и океана. 1981. Т. 17, № 7. С. 732–736.
9. *Долин Л.С.*, *Левин И.М.* Справочник по теории подводного видения. Л. Гидрометеоиздат, 1991. 230 с.
10. *Dolin L.*, *Gilbert G.*, *Levin I.*, *Luchinin A.* Theory of imaging through wavy sea surface. N. Novgorod: Institute of Applied Physics, 2006. 180 p.
11. *Левин И.М.* О наблюдении объектов, освещенных узким световым пучком, в рассеивающей среде // Известия АН СССР. Физика атмосферы и океана. 1969. Т. 5, № 1. С. 62–76.
12. *Браво-Животовский Д.М.*, *Долин Л.С.*, *Лучинин А.Г.*, *Савельев В.А.* Некоторые вопросы теории видения в мутных средах // Известия АН СССР. Физика атмосферы и океана. 1969**.** Т. 5, № 7. С. 672–684.
13. *Вебер В.Л.*, *Лучинин А.Г.* Влияние корреляционных эффектов на характеристики изображения дна водоема, наблюдаемого через взволнованную поверхность // Известия АН СССР. Физика атмосферы и океана. 2001. Т. 37, № 2. С. 257–264.
14. *Walker R.E.* Marine Light Field Statistics. John Wiley&Sons, INC. 1994. 675 p.
15. *Luchinin A.G.*, *Kirillin M. Yu.* Nonstationary optical transfer functions of underwater imaging systems // Applied Optics. 2017. Vol. 56, N 27. P. 7518–7524. doi:10.1364/AO.56.007518
16. *Dolin L.S.*, *Luchinin A.G.* Water-scattered signal to compensate for the rough sea surface effect on bottom lidar imaging // Applied Optics. 2008. Vol. 47, N36. P. 6871–6878. doi:10.1364/ao.47.006871
17. *Лучинин А.Г.*, *Долин Л.С.* Модель системы подводного видения со сложно модулированным пучком подсветки // Известия РАН. Физика атмосферы и океана. 2014. Т. 50, № 4. С. 468–476. doi:10.7868/S0002351514040099

About the authors

Aleksandr G. Luchinin	Dr.Sci. (Phys.-Math.), Chief Researcher, Federal Research Center Institute of Applied Physics of the Russian Academy of Sciences (603950, Ul'anova str., 46, Nizhny Novgorod, Russia)	elibrary AuthorID: 472 e-mail: luch@ipfran.ru
Mikhail Yu. Kirillin	Ph.D. (Phys.-Math.), Senior Researcher, Federal Research Center Institute of Applied Physics of the Russian Academy of Sciences (603950, Ul'anova str., 46, Nizhny Novgorod, Russia)	ORCID ID 0000-0002-6804-6369, elibrary AuthorID: 153037, e-mail: kirillin@ipfran.ru